Purdue University
Purdue e-Pubs

Birck and NCN Publications | Birck Nanotechnology Center

12-4-2008

Optical hyperspace for plasmons: Dyakonov states in metamaterials

Zubin Jacob
Birck Nanotechnology Center, Department of Electrical and Computer Engineering, Purdue University, zjacob@purdue.edu

Evgenii E. Narimanov
Birck Nanotechnology Center, Department of Electrical and Computer Engineering, Purdue University, evgenii@purdue.edu

Follow this and additional works at: http://docs.lib.purdue.edu/nanopub

 Part of the Nanoscience and Nanotechnology Commons

Jacob, Zubin and Narimanov, Evgenii E., "Optical hyperspace for plasmons: Dyakonov states in metamaterials" (2008). *Birck and NCN Publications.* Paper 334.
http://docs.lib.purdue.edu/nanopub/334

This document has been made available through Purdue e-Pubs, a service of the Purdue University Libraries. Please contact epubs@purdue.edu for additional information.

Optical hyperspace for plasmons: Dyakonov states in metamaterials

Zubin Jacob[a] and Evgenii E. Narimanov
Birck Nanotechnology Center, Department of Electrical and Computer Engineering, Purdue University, West Lafayette, Indiana 47906, USA

(Received 30 September 2008; accepted 5 November 2008; published online 4 December 2008)

We show that the subdiffraction imaging behavior observed in the magnifying superlens experiment, [Smolyaninov *et al.*, Science **317**, 1699 (2007)] is due to the hyperbolic dispersion of Dyakonov plasmons supported by the device. These states which are a special case of Dyakonov surface waves [Dyakonov, Sov. Phys. JETP **67**, 714 (1988)] exist at the interface of a metal and an anisotropic dielectric giving rise to plasmon beams on resonance. Furthermore, we describe how the unique properties of metamaterial Dyakonov plasmons can be tailored for plasmonic devices. © *2008 American Institute of Physics*. [DOI: 10.1063/1.3037208]

Surface plasmons, which are collective charge oscillations on the surface of metals, have found applications as varied as light manipulation at the nanoscale to single molecule biosensing[1]. The unconventional properties of such surface plasmons at the interface of a negative index metamaterial[2] and a positive index medium have been the subjects of recent theoretical[3,5] and experimental interest.[6] In particular, the ability of the superlens to surpass the diffraction barrier is attributed to the degenerate plasmon resonance of a slab made with left handed material.[4]

Recently an imaging system consisting of a metal substrate with concentric dielectric rings on top, called the magnifying superlens, was demonstrated to achieve subwavelength resolution along with magnification.[7] However, with this nontrivial geometry, it is not apparent whether the device supports the degenerate plasmon spectrum as in the conventional superlens. Furthermore the absence of magnetism makes it unclear how the structure is similar to the superlens which has $\epsilon<0$ and $\mu<0$. Another intriguing aspect has been the observation of unique subdiffraction beams in the subwavelength imaging regime which is not characteristic of the conventional superlens. This warrants a deeper investigation into the mechanism of subwavelength imaging in the magnifying superlens.

In the present paper, we show that the subwavelength imaging in the magnifying superlens originates from hyperbolic isofrequency curves of light propagating in the device. This is also the key property behind the operation of another metamaterial device, the hyperlens. The latter is a device which breaks the diffraction limit using the bulk dielectric properties of a metamaterial medium and projects an image with subwavelength details into the far field.[8,9] A hyperbolic isofrequency curve is crucial to the subdiffraction imaging behavior of the hyperlens which is achieved by a metamaterial with dielectric constants of opposite signs in opposite directions.[10] Large wavevectors containing subwavelength information decay in a normal medium such as vacuum but are supported in the metamaterial medium comprising the hyperlens due to its hyperbolic isofrequency curve. As we will describe in this paper, the hyperbolic isofrequency curve in the magnifying superlens structure arises due to the Dyakonov plasmons at the interface of a metal and anisotropic dielectric in contrast to the bulk wavevectors in a strongly anisotropic metamaterial. Furthermore a flat isofrequency curve can be achieved which facilitates subdiffraction imaging using these Dyakonov states.

Dyakanov surface waves unlike surface plasmons can occur at the interface between two dielectric media, at least one of which has to be anisotropic.[11] The specific requirement for their excitation makes an experimental observation difficult and structures which are amenable to Dyakonov surface wave excitation and detection have been recently suggested.[12,13] In this paper, we show that the properties observed in Ref. 7 are explained by the existence of Dyaknov plasmons on the interface of the metal and effective medium formed by the dielectric ring structure on top. We thus demonstrate that the investigation in Ref. 7 was an experimental observation of Dyakonov surface states.

The magnifying superlens structure[7] consists of concentric dielectric rings of PMMA deposited on a gold film surface. The plasmon beams occur in a narrow frequency interval near 495 nm and away from this resonance there is no beaming or subwavelength imaging. The medium on top of the gold film surface comprising of air voids and PMMA rings can be described as an effective medium if the width of each ring fabricated on the metal substrate is smaller than the wavelength. In this limit the dielectric ring pattern corresponds to a cylindrically anisotropic dielectric. We therefore model the behavior of plasmons in the magnifying superlens structure by considering a metal (ϵ_m) with an anisotropic dielectric on top which has a dielectric tensor given by $\epsilon=\mathrm{diag}(\epsilon_\parallel,\epsilon_\perp,\epsilon_\perp)$, where $\epsilon_\parallel=(\epsilon_d.1)/(1.d_{\mathrm{PMMA}}+\epsilon_d d_{\mathrm{air}})$ and $\epsilon_\perp=(\epsilon_d d_{\mathrm{PMMA}}+d_{\mathrm{air}}.1)/(d_{\mathrm{PMMA}}+d_{\mathrm{air}})$. The direction parallel and perpendicular is with respect to the optic axis.

The original paper by Dyakonov considered the interface of two dielectrics, one of which was anisotropic and the work of Crasovan *et al.*[14] extended this treatment to negative index materials. Here we consider the plasmonic equivalent of such surface states that can occur on the interface of a metal and anisotropic dielectric, which we refer to as Dyakonov plasmons. When the optic axis of the dielectric is oriented perpendicular to the interface plane, this structure can also support regular plasmons, recently suggested for use in scattering-free plasmonic devices.[15] Our focus is on Dyakonov plasmons, a special case of Dyakonov surface states which emerge when the optic axis lies in the interface plane, as shown in Fig. 1(a). These are mixed polarization surface states characterized by three decay constants, two

[a]Electronic mail: zjacob@purdue.edu.

 © 2008 American Institute of Physics

Downloaded 19 Feb 2009 to 128.46.220.88. Redistribution subject to AIP license or copyright; see http://apl.aip.org/apl/copyright.jsp

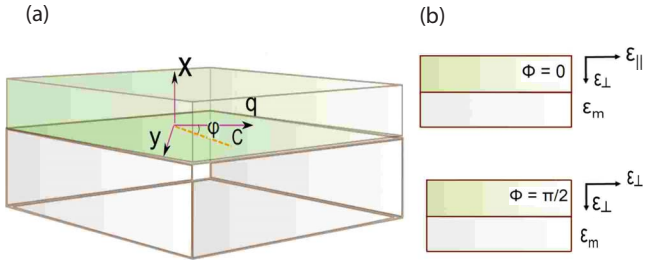

FIG. 1. (Color online) (a) Schematic of the structure modeling the magnifying superlens, uniaxial crystal on a metal substrate. The plasmon wavevector makes an angle ϕ with the optic axis (C) of the uniaxial crystal. (b) (Top) Parallel-plasmon in a direction parallel to the optic axis ($\phi=0$); (Bottom) perpendicular plasmon ($\phi=\pi/2$).

corresponding to the ordinary and extraordinary wave in the uniaxial crystal and one corresponding to the decay in the metal. The field in the metal shows both TE and TM characters unlike the plasmon on the boundary of a metal and isotropic dielectric which is of TM nature. The boundary conditions following Dyakonov's original ansatz can be written in the general form $\alpha^m_{\mathrm{TE}}X_{\mathrm{TE}}+\alpha^m_{\mathrm{TM}}X_{\mathrm{TM}}=\alpha^{\mathrm{xtal}}_{(e)}X_{(e)}+\alpha^{\mathrm{xtal}}_{(o)}X_{(o)}$, where $(\alpha^m_{\mathrm{TE}},\alpha^m_{\mathrm{TM}})$ denote the contributions of the TE and TM polarizations in the metal and $[\alpha^{\mathrm{xtal}}_{(e)},\alpha^{\mathrm{xtal}}_{(o)}]$ correspond to the contribution of the (e)-wave and (o)-wave in the crystal to the Dyakonov state. The consistency of the four boundary conditions corresponding to the continuity of $X\equiv(E_z,E_y,B_z,B_y)$ gives rise to the dispersion relation, $\det(\Delta(q,k_1,k_2,k_3,\phi))=0$ where,

$$\Delta=\begin{vmatrix} \epsilon_\perp\sin(\phi) & ik_3 & 0 & 1 \\ (\epsilon_\perp-q^2)\cos(\phi) & ik_3\sin(\phi) & ik_1 & 0 \\ ik_2\epsilon_\perp\sin(\phi) & k_3^2\cos(\phi) & 0 & -ik_1 \\ ik_2\epsilon_\perp\cos(\phi) & \epsilon_\perp\sin(\phi) & -\epsilon & 0 \end{vmatrix}. \quad (1)$$

The Dyakonov plasmon wavevector q makes an angle ϕ with the optic axis, the decay constant in the metal is k_1 while the decay constants in the anisotropic dielectric are k_2 and k_3 for the (e)-wave and (o)-wave, respectively. Any practical realization of a Dyakonov plasmon supporting structure must have an anisotropic crystal thickness larger than the decay lengths of the extraordinary wave as well as the ordinary wave. The direction of the z-axis is chosen to coincide with the wavevector. Note that the eigenvectors corresponding to the null eigenvalue of Δ determine the contribution $(\alpha^m_{\mathrm{TE}},\alpha^m_{\mathrm{TM}},\alpha^{\mathrm{xtal}}_{(e)},\alpha^{\mathrm{xtal}}_{(o)})$ of the polarizations to the Dyakonov plasmon. Along with the consistency condition the wavevector components have to satisfy the following dispersion relations in the metal, $q^2-k_1^2=\epsilon_m k_0^2$, while for the (e)-wave and (o)-wave in the uniaxial crystal, we have $(q^2\sin^2(\phi)/\epsilon_\parallel)+(q^2\cos^2(\phi)/\epsilon_\perp)-(k_2^2/\epsilon_\parallel)=k_0^2$ and $q^2-k_3^2=\epsilon_\perp k_0^2$. Using the above equations, we can solve for the decay constants and propagation vector as a function of angle. As expected from the in-plane anisotropy, the Dyakonov plasmon has a wavevector which varies with angle ϕ from the optic axis of the uniaxial crystal. The Dyakonov plasmons for the two high symmetry directions degenerate into the normal TM plasmons on a metal-dielectric interface as the eigenvector components $\alpha^m_{\mathrm{TE}}=0$ and $\alpha^{\mathrm{xtal}}_{(e)}=0$ when ϕ is 0 or $\pi/2$, i.e., the contribution to the Dyaknov plasmon of the TE polarization in the metal and the (e)-wave in the crystal vanishes. (The plasmons in these two directions will

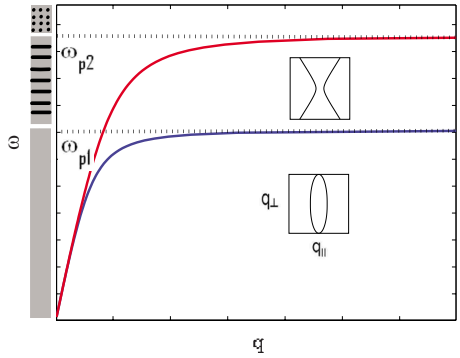

FIG. 2. (Color online) Dispersion curve of the plasmons along the high symmetry directions for the zero loss case. The region in gray denotes frequencies when both the plasmons exist; the dashed region corresponds to frequencies when only one plasmon exists whereas for frequencies in the dotted region, neither plasmon exists. The insets describe the nature of the isofrequency curve expected in each frequency region.

be referred to as the parallel plasmon ($\phi=0$) and perpendicular Plasmon, respectively ($\phi=\pi/2$) [Fig. 1(c)]. The wavevector for the perpendicular-plasmon is simply $q_\perp=k_0\sqrt{\epsilon_m\epsilon_\perp/\epsilon_m+\epsilon_\perp}$, whereas for the parallel-plasmon it is given by $q_\parallel=k_0\sqrt{\epsilon_\parallel\epsilon_m(\epsilon_\perp-\epsilon_m)/\epsilon_\parallel\epsilon_\perp-\epsilon_m^2}$.

Now we describe the isofrequency curves of Dyakonov plasmons which are supported by the structure of Fig. 1. To simplify the qualitative analysis, we, neglect losses, but the extension of this discussion to include finite losses is straightforward.[1] As described above, the Dyakonov plasmons in two high symmetry directions degenerate into regular plasmons which have dispersion curves, as shown in Fig. 2. The gray shaded region in Fig. 2 denotes frequencies where both regular plasmons exist and by continuity we expect the Dyakonov plasmon solution to be found for an arbitrary direction in the interface plane leading to a closed isofrequency curve. In the range of frequencies indicated by the dashed gray area in Fig. 2, only one of the two regular plasmons exists; hence the Dyakonov plasmon occurs only within a narrow range of angles. This narrow range is expected to be centered around the high symmetry direction along which the regular plasmon exists and the isofrequency curve will necessarily be an open curve. Neither of the two regular plasmons occur at frequencies in the dotted gray region of Fig. 2. We thus do not expect Dyakonov plasmons to exist at these frequencies for any angle. For a frequency chosen within the gray shaded region of Fig. 2, the variation of the Dyakonov wavevector with angle is plotted in Fig. 3(a) and indeed the isofrequency curve is shaped like an ellipse [Fig. 3(b)]. The angular wavevector variation and isofrequency curve for a frequency lying in the dashed gray region of Fig. 2 are shown in Fig. 4. Unlike the previous case, Dyakonov plasmon solutions can be found only within a narrow range of angles. Note that the wavenumber diverges at the boundaries of this range and the isofrequency curve is shaped like a hyperbola Fig. 4(b). As is intuititvely expected, the in-plane anisotropy has given rise to a directional Dyakonov plasmon resonance.

The transition when the isofrequency curve changes from an elliptical shape to hyperbolic occurs at the plasmon resonance frequency of one of the high symmetry plasmons. Near this transition frequency, we have a flat isofrequency curve which is the regime where the magnifying superlens functions as a subdiffraction imaging system. The flat

Downloaded 19 Feb 2009 to 128.46.220.88. Redistribution subject to AIP license or copyright; see http://apl.aip.org/apl/copyright.jsp

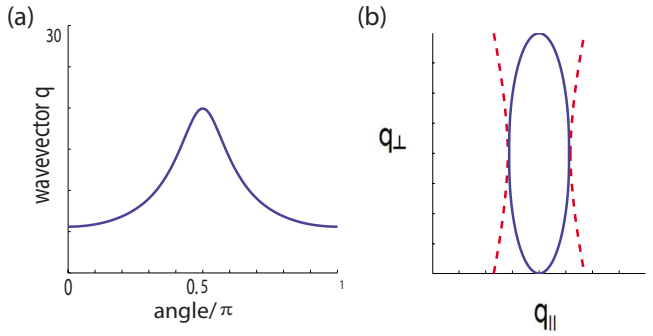

FIG. 3. (Color online) (a) Variation of the Dyakonov plasmon wavevector with angle; the curve corresponds to the case when the frequency is close to the perpendicular-plasmon resonance causing a larger value of the wavevector at $\phi=\pi/2$. (c) Ellipse shaped isofrequency curve and transition to hyperbolic shaped isofrequency curve beyond the perpendicular-plasmon resonance.

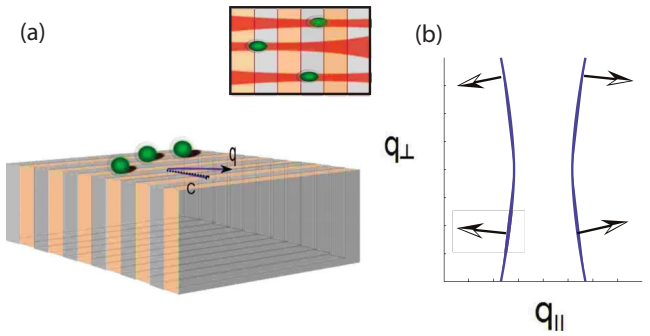

FIG. 5. (Color online) (a) Schematic of a quantum dot emitter on an anisotropic metal structure made of alternating subwavelength layers of metal and dielectric (inset) top view of the directional emission from each emitter. (b) Hyperbolic isofrequency curve of the Dyakonov plasmons on the anisotropic metal with arrows denoting the Poynting vectors.

isofrequency curve shown in Fig. 3(b) occurs close to the perpendicular plasmon resonance condition $[\epsilon_m(\omega)+\epsilon_\perp=0]$. Note that the wavevector value peak in Fig. 3(a) occurs at $\phi=\pi/2$ since the chosen frequency is near the perpendicular plasmon resonance condition. A similar flat isofrequency curve can also be achieved at the parallel-plasmon resonance condition $[\epsilon_m(\omega)=-\sqrt{\epsilon_\parallel\epsilon_\perp}]$. The above analysis shows that Dyakonov plasmons demonstrate all the general features characteristic of propagating waves in a medium with hyperbolic isofrequency curves. Thus the magnifying superlens structure which supports these Dyakonov plasmons is functionally similar to the hyperlens which explains the far field subwavelength imaging. The origin of subdiffraction plasmon beams in the magnifying superlens is also the flat isofrequency curve. Normals to the isofrequency curve give the direction of Poynting vectors, i.e., energy flow direction of the plasmon on the interface plane. For the flat isofrequency curve corresponding to the Dyakonov plasmons, all the Poynting vectors point in the same direction leading to a subdiffraction resonance cone beam.[16,17] A hyperbolic isofrequency curve necessarily implies that the plasmon Poynting vectors will lie within a cone but the cone collapses to a subdiffraction beam only when the isofrequency curve is flat.

The structure used to model the magnifying superlens supports Dyakonov plasmon states but accessing the interface states of a metal and uniaxial crystal offers less flexibility with regard to applications such as surface enhanced sensing. To circumvent this limitation and also investigate other possible applications, we now turn our attention to an anistropic metal substrate ($\epsilon_\perp<0$, $\epsilon_\parallel>0$) which supports Dyakonov plasmons with similar properties as described above (for metamaterial realization see Ref. 18). A unique feature of Dyakonov plasmons is the directional resonance useful for sensing [Fig. 4(a)]. This preferred angular direction, along which the wavevector of Dyakonov plasmons takes on large values, is given by $[\phi_0,\pi-\phi_0]$, where $\phi_0=\arcsin\sqrt{(\epsilon_d^2-\epsilon_\parallel\epsilon_\perp)/\epsilon_\perp(\epsilon_\perp-\epsilon_\parallel)}$ and $\epsilon_d=1$ is the permittivity of the dielectric on top of the anisotropic metal. Sources of radiation, such as quantum dots placed on the anisotropic metal substrate can couple to Dyakonov plasmon states which will lead to highly directional and tightly confined plasmon beams [Fig. 5(a)]. The Poynting vectors shown in Fig. 5(b) define the boundary of the narrow resonance cone within which the light is emitted leading to a collective directional emission of Dyakonov plasmon beams by every quantum dot.

In conclusion, we have shown that the subwavelength imaging in Ref. 7 is due to Dyakonov plasmons. This work was partially supported by ARO-MURI Award No. 50342-PH-MUR.

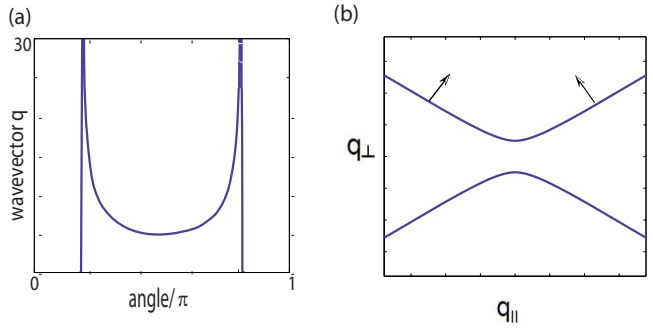

FIG. 4. (Color online) (a) Wavevector variation with angle on the interface plane measured from the optic axis. Note that the wavevector takes on large values only in a specific direction. (b) Hyperbolic isofrequency curve of the Dyakonov plasmon with the arrows denoting the Poynting vectors, i.e., direction of energy flow of the Dyakonov plasmon.

[1] H. Raether, *Surface Plasmon on Smooth and Rough Surfaces and on Gratings* (Springer, New York, 1988).
[2] V. G. Veselago, Sov. Phys. Usp. **10**, 509 (1968).
[3] J. B. Pendry, Phys. Rev. Lett. **85**, 3966 (2000).
[4] F. D. M. Haldane, arXiv:cond-mat/0206420.
[5] R. Ruppin, Phys. Lett. A **277**, 61 (2000).
[6] N. Fang, H. Lee, C. Sun, and X. Zhang, Science **308**, 534 (2005).
[7] I. Smolyaninov, Y. Hung, and C. Davis, Science **315**, 1699 (2007).
[8] Z. Jacob, L. V. Alekseyev, and E. Narimanov, Opt. Express **14**, 8247 (2006).
[9] A. Salandrino and N. Engheta, Phys. Rev. B **74**, 075103 (2006).
[10] Z. Liu, H. Lee, Y. Xiong, C. Sun, and X. Zhang, Science **315**, 1686 (2007).
[11] M. I. Dyakonov, Sov. Phys. JETP **67**, 714 (1988).
[12] D. Artigas and L. Torner, Phys. Rev. Lett. **94**, 013901 (2005).
[13] A. Lakhtakia and J. A. Polo, Jr., J. Eur. Opt. Soc. Rapid Publ. **2**, 07021 (2007).
[14] L. C. Crasovan, O. Takayama, D. Artigas, S. K. Johansen, D. Mihalache, and L. Torner, Appl. Phys. Lett. **92**, 141115 (2008). A similar ansatz has been recently rediscovered in Appl. Phys. Lett. **92**, 141115 (2008).
[15] J. Elser and V. Podolskiy, Phys. Rev. Lett. **100**, 066402 (2008).
[16] E. Arbel and L. B. Felsen, in *Electromagnetic Theory and Antennas*, edited by E. C. Jordan (Pergamon, New York, 1963).
[17] Z. Jacob, L. V. Alekseyev, and E. Narimanov, J. Opt. Soc. Am. A **24**, A52 (2007).
[18] V. A. Podolskiy and E. E. Narimanov, Phys. Rev. B **71**, 201101 (2005).

Downloaded 19 Feb 2009 to 128.46.220.88. Redistribution subject to AIP license or copyright; see http://apl.aip.org/apl/copyright.jsp